Integration of Air Classification and Hydrothermal Carbonization to Enhance Energy Recovery of Corn Stover

March 2021

Md Tahmid Islam, Nepu Saha, M. Toufiq Reza, Jordan L Klinger, Sergio Hernandez

Changing the World's Energy Future

INL
Idaho National Laboratory

Integration of Air Classification and Hydrothermal Carbonization to Enhance Energy Recovery of Corn Stover

Md Tahmid Islam, Nepu Saha, M. Toufiq Reza, Jordan L Klinger, Sergio Hernandez

March 2021

Idaho National Laboratory
Idaho Falls, Idaho 83415

http://www.inl.gov

Integration of Air Classification and Hydrothermal Carbonization to Enhance Energy Recovery of Corn Stover

Md Tahmid Islam [1], Nepu Saha [1], Sergio Hernandez [2], Jordan Klinger [2] and M. Toufiq Reza [1,*]

[1]   Department of Biomedical and Chemical Engineering and Sciences, Florida Institute of Technology, 150 W University Boulevard, Melbourne, FL 32901, USA; islamm2019@my.fit.edu (M.T.I.); nsaha2019@my.fit.edu (N.S.)

[2]   Biomass Characterization Department, Idaho National Laboratory, 2525 Fremont Ave, Idaho Falls, Idaho, ID 83402, USA; sergio.hernandez@inl.gov (S.H.); jordan.klinger@inl.gov (J.K.)

[*]   Correspondence: treza@fit.edu; Tel.: +1-321-674-8578

Abstract: Air classification (AC) is a cost-effective technology that separates the energy-dense light ash fraction (LAF) from the inorganic-rich high ash fraction (HAF) of corn stover. HAF could be upgraded into energy-dense solid fuel by hydrothermal carbonization (HTC). However, HTC is a high-temperature, high-pressure process, which requires additional energy to operate. In this study, three different scenarios (i.e., AC only, HTC only, and integrated AC–HTC) were investigated for the energy recovery of corn stover. AC was performed on corn stover at an 8 Hz fan speed, which yielded 84.4 wt. % LAF, 12.8 wt. % HAF, and 2.8 wt. % below screen particles. About 27 wt. % ash was reduced from LAF by the AC process. Furthermore, HTC was performed on raw corn stover and the HAF of corn stover at 200, 230, and 260 °C for 30 min. To evaluate energy recovery, solid products were characterized in terms of mass yield, ash yield, ultimate analysis, proximate analyses, and higher heating value (HHV). The results showed that the energy density was increased with the increase in HTC temperature, meanwhile the mass yield and ash yield were decreased with the increase in HTC temperature. Proximate analysis showed that fixed carbon increased 18 wt. % for original char and 27 wt. % for HAF char at 260 °C, compared to their respective feedstocks. Finally, the hydrochar resulting from HAF was mixed with LAF and pelletized at 180 bar and 90 °C to densify the energy content. An energy balance of the integrated AC–HTC process was performed, and the results shows that integrated AC with HTC performed at 230 °C resulted in an additional 800 MJ/ton of energy recovery compared to the AC-only scenario.

Keywords: corn stover; air classification; hydrothermal carbonization; pelletization; energy recovery

1. Introduction

More than one billion tons of biomass will be available for bioenergy production in the USA by 2030 [1–3]. Among other resources, corn stover (CS) has a huge potential to contribute to the renewable energy portfolio, as more than 250 million dry tons of CS are produced annually in the USA [1,4]. With proper feedstock handling and preprocessing, CS could become an abundant source of bioenergy [5,6]. However, a significant amount of agricultural waste, including CS, is burnt or left unprocessed in the field due to high logistical costs. This results in serious environmental problems and economic forfeiture [7,8]. Therefore, the utilization of potential bioenergy from waste biomass sources such as CS needs to be considered with urgency.

Air classification (AC) is a low-cost preprocessing technology that has been developed particularly in agricultural processing and mining applications. In AC, the separations are performed based on a combination of material size, density, and drag properties, utilizing screens and air streams to effectively separate high-density fractions from low-density fractions. In general, large amounts of soil, rocks, and other foreign matters are incorporated into the feedstock during harvest and collection. The inorganics, dirt, rocks,

and foreign materials are mostly dense materials compared to the lignocellulosic structure of biomass. Therefore, AC separates a significant amount of these exogenous inorganics and creates an enriched stream of biomass (often called the light ash fraction, LAF) and a soil-laden reject stream (also known as the high ash fraction, HAF) [9–11]. Lacey et al. [11] showed such separations for chipped forest residues after AC and reported remarkable ash (wt. %) reductions (>32 wt. %) in the final throughputs. Emerson et al. [9] also found quite reasonable reductions in ash (wt. %) for hybrid poplar (from 2.34 wt. % to 1.67 wt. %) and shrub willow (from 2.60 wt. % to 2.14 wt. %). Recently, Thompson et al. [2] showed that AC can effectively upgrade CS by removing 30 wt. % ash at a mild 7.5 Hz fan speed, or approximately 2.1 m/s counter-stream air flow of AC. It has also been reported that a large fraction of HAF byproduct is produced during AC, accounting for more than 12 wt. % of the initial CS. This HAF of CS contains more than 80 wt. % organic content that can be further utilized [2]. Instead, an estimated HAF disposal cost of USD 28.86 per ton has been suggested by Reza et al. [12] and Humbird et al. [13], accounting for 2.5 cents of the USD 2.15 per gallon minimum ethanol selling price. In order to make AC more economically viable, the further utilization of HAF needs to be implemented in conjunction with AC technologies and system-wide economics and sustainability for full material utilization. However, to the best of the authors' knowledge, no work has been done to date to utilize the waste energy in value-added fuel. Therefore, to make use of the vital unrecovered energy from this solid waste and integrate it with the AC technology, the HAF could be converted into essential products.

Hydrothermal carbonization (HTC) is a promising thermochemical process that transforms biomass, such as CS, into a carbon-rich solid product called hydrochar [5,14,15]. The reaction temperature varies between 180 and 260 °C, and the pressures are maintained above the saturation pressure. The ionic products of water increase three orders of magnitude ($K_{H2O\ (573K)}/K_{H2O\ (298K)} = 10^3$) [5,15,16] and the dielectric constant of water reduces from 78.5 (298 K, 0.1 MPa) to 27.1 (523 K, 5 MPa) [15,17]. As a result, biomass undergoes a series of reactions, i.e., hydrolysis, decarboxylation, dehydration, condensation polymerization, and aromatization, in subcritical water due to the increased reactivity and solvent-like properties [18,19]. For agricultural residues, the HTC reaction products can be divided into three streams: 41–90 wt. % solids with 80–95 wt. % of the original calorific value; 2–10 wt. % gas consisting mainly of CO_2; the rest is process liquid [20–24]. The energy-dense solid hydrochar can be pelletized to improve the mass and energy density of the feedstock and reduce the cost of transportation, handling and storage [25–27].

During HTC, the low density and low viscosity of subcritical water, in combination with the acidic process liquid and the modification of the biomass structure, aid in the leaching of inorganics from biomass structures [18,28–31]. The reduction of ash is particularly important for hydrochars' application as fuel, as this can significantly reduce the ash-fusion temperatures, leading to slagging in fuel boilers [1]. Therefore, HTC could be used to recover the energy in the HAF stream while reducing ash from the hydrochar. However, HTC is an energy-intensive process as it requires high temperatures and high pressure. Therefore, an energy balance in the integrated AC–HTC is warranted to evaluate the net energy recovery from the integrated process compared to the individual AC and HTC processes. Therefore, the main goal of this work was to study the feasibility of three different scenarios, to determine the energy recovery from CS: 1. AC-only process; 2. HTC-only process; 3. Integrated AC–HTC process. First, the AC of CS was performed to separate LAF and HAF. Then HTC on HAF was performed at various temperatures and the hydrochars were pelletized with LAF. The energy recovery from the integrated AC–HTC process was compared with AC-only and HTC-only, wherein the original (ORG) CS was used for both technologies.

2. Materials and Methods

2.1. Materials

A raw corn stover bale from Kadolph Farms in Hardin, Iowa was deconstructed in the process development unit (PDU) of the Idaho National Laboratory's Biomass Feedstock National User Facility (BFNUF). The bale was harvested in the fall of 2018 using an 8-row stripper header and raked using rotary tedder prior to baling. Bales were stored immediately after baling in stacks at the field edge with a six-high by three-length stacking position. Size reduction in the BFNUF was accomplished using a Vermeer prototype horizontal bale grinder (BG480, Pella, Iowa) with a 15.24 cm screen. This mill was powered by two 200 HP electric motors with 96 swinging hammers on each of the two grinding drums. The sample, referred to as ORG CS hereafter, was dried below 10 wt. % moisture content prior to AC and HTC treatments.

2.2. Methods

2.2.1. Air Classification of Corn Stover

The ORG CS intended for HTC were sampled using mechanical sampling procedures and equipment according to Solid Biofuels Sampling ISO 18135:2017. A super sack of the deconstructed CS bale was divided using a custom rotary splitter that consists of a conveyor and eight bins mounted on a rotating table. In this unit, a feed hopper accommodates approximately 120 L of sample and a live-bottom style belt feeder slowly dispenses the samples to 8 sample bins below. The 45 L bins rotate over 100 times during each splitting operation and make at least one full rotation for each belt flight to ensure the samples are representative of the original bulk solid. Both the belt feeder and the rotary table are equipped with speed control devices (variable frequency drive and/or DC potentiometer) to adjust the processing parameters according to the sample feed behavior to ensure analytical splitting (an image of AC can be found in the supplementary information (Figure S1)). AC separates the samples into two fractions as the material is passed over a screen-covered fan: LAF and HAF. The HAF is blown upward and removed while the LAF (air classified material) remains. Air classification was performed on CS feedstocks using a 2× Air Cleaner equipped with an Iso-flo dewatering infeed shaker (Key Technologies, Walla Walla, WA, USA). CS was air classified using a fan speed of 1.8 m/s. Both light and heavy fractions were collected after classification for downstream processing and analyses.

2.2.2. Hydrothermal Carbonization (HTC)

HTC was carried out in the 300 mL Parr reactor (Moline, IL, USA) for 30 min at three different temperatures 200, 230, and 260 °C (an image of the HTC reactor system is shown in the supplementary section (Figure S2)). In a typical HTC run, 20 g of dry CS (HAF or ORG CS) was mixed with 180 mL of deionized (DI) water inside the reactor vessel. The reactor was stirred at 150 ± 5 rpm throughout the HTC experiment. The temperature of the reactor was controlled using a proportional integral derivative (PID) controller. The heating rate was maintained at 10 °C min^{-1}. The pressure was not controlled but monitored throughout the HTC, which was found to be 210 ± 20 psi, 380 ± 20 psi, and 620 ± 20 psi for the 200 °C, 230 °C and 260 °C operating temperatures, respectively. When the reactor reached the desired HTC temperature, it was kept isothermal for 30 min. At the end of the HTC reaction time, the heater was turned off and the reactor was quenched by an ice water bath. It took 15 ± 5 min to cool down the reactor below 50 °C. The gas produced during HTC was not the focus of this work and was vented in a fume hood. The slurry was then filtered using Whatman 41 filter paper in a vacuum filtration system. The hydrochar was first washed with approx. 200 mL deionized (DI) water to remove the HTC liquid products that adhered to the hydrochar, and then dried at 105 °C for 24 h in an oven. The dried hydrochar was stored in a ziplock bag for further analysis. The solid mass yield (MY) was calculated using Equation (1). Each hydrochar referred to in this work is

labeled according to the HTC temperature. For instance, CS ORG HTC200 represents the hydrochar produced from ORG CS at 200 °C.

$$MY(wt.\,\%) = \frac{\text{Mass of dried post(g)} - \text{process solid(g)}}{\text{Mass of untreated dry feedstock (g)}} \times 100\% \tag{1}$$

2.2.3. Pelletization of Hydrochar with Corn Stover

Samples (LAF, ORG hydrochar, and hydrochar–LAF mix) were pelletized using a 24 ton benchtop single-press pellet press (Across International, model # MP24A, Livingston, NJ) (an image of the pellet press can be found in the supplementary information (Figure S3)). About 1.5 g of dry sample was powdered using mortar pestle to make it homogeneous. From the homogeneous powdered sample, 0.50 g of dry was taken out and put in the die sleeve of the 13 mm circular pressing die. A compressive force of 7.5 MT was applied at the top surface of the sample by the lever. The temperature was set at 90 °C (beyond the glass transition temperature for CS) [32] using a band heater and the holding time was set at 30 s for each pellet. Pellets were stored in sealed bags for further characterizations.

2.3. Product Characterization
2.3.1. Higher Heating Value (HHV)

An IKA C 200 bomb calorimeter (Staufen, BW, Germany) was used to determine higher heating values (HHV) of the raw and hydrochar pellets by following the ASTM D240 method. Energy yield (EY) was calculated by Equation (2). Triplicates were performed for each sample to report reproducibility.

$$EY(\%) = MY(wt.\,\%) \times \frac{\text{HHV of dried hydrochar } \left(\frac{MJ}{kg}\right)}{\text{HHV of untreated dry feedstock } \left(\frac{MJ}{kg}\right)} \tag{2}$$

2.3.2. Ash

The ASTM D1102 method was followed to determine the ash content of the dry solid samples by using a muffle furnace (Thermo Scientific, Model # FB1415M, Waltham, MA) at 575 °C for 5 h 30 min. The ash yield (AY) was calculated by using Equation (2). Triplicates were performed for each sample to report reproducibility.

$$AY\,(wt.\,\%) = MY(wt.\,\%) \times \frac{\text{Ash in hydrochar (wt.\,\%)}}{\text{Ash in raw feedstock (wt.\,\%)}} \tag{3}$$

2.3.3. Thermogravimetric Analysis (TGA)

The volatile matter (VM) and fixed carbon (FC) of samples were determined by TGA using a TGA Q5000 (TA instruments, New Castle, DE, USA). The experimental procedure was taken from the literature [33]. Experiments were carried out under inert atmosphere using a constant flowrate (10 mL/min) of nitrogen to avoid any possible oxidation and to continuously purge the VM. The sample was first heated to 105 °C and kept isothermal for 5 min. The mass loss at this temperature accounts for the moisture content (MC). The sample was then heated to 900 °C at a ramp rate of 20 °C/min and kept isothermal for 5 min. The mass loss from 105 °C to 900 °C accounts for VM. Finally, the FC (wt. %) was then calculated from Equation (3):

$$FC\,(wt.\,\%) = 100\,wt.\,\% - MC\,(wt.\,\%) - VM\,(wt.\,\%) - ash\,(wt.\,\%) \tag{4}$$

2.3.4. CHNS/O Analysis

A FLASH EA 1112 Series (Thermo Scientific, Waltham, MA, USA) elemental analyzer was used to quantify the elemental carbon (C), hydrogen (H), nitrogen (N), and sulfur (S) content in the sample using the method described in the literature [34]. For the analysis, 2, 5-Bis (5-tert-butyl-benzoxazol-2-yl) thiophene (BBOT) was used as a calibration standard

and vanadium oxide (V_2O_5) as a conditioner for the samples, which were combusted around 950 °C in ultra-high purity oxygen with helium carrier gas and passed over copper oxide pellets and then electrolytic copper. The produced gases were then analyzed by a thermal conductivity detector (TCD), with the peak areas of detection being compared to those of BBOT standards. The oxygen (O) content was found by subtraction method. The following equation was used to find the oxygen wt. %.

$$O \text{ (wt. \%)} = 100 \text{ wt. \%} - C \text{ (wt. \%)} - H \text{ (wt. \%)} - N \text{ (wt. \%)} - S \text{ (wt. \%)} - \text{ash (wt. \%)} \quad (5)$$

3. Results and Discussion

3.1. Characterization of Air Classified CS

The AC of ORG CS led to an LAF or "clean" fraction and an HAF or "dirty" fraction. All the separations were conducted under the fan speed and frequency of 1.8 m/s and 8 Hz, respectively. These conditions were chosen for optimum separation as reported in the literature [2,9,11,35]. As seen in Figure 1, the separated LAF contains more low ash plant tissue fractions such as cobs, stalks, and husks, while the HAF contains more of the undesired plant fractions (leaves, pith, rind) that usually contain higher ash values as well as soil entrained during plant growth or picked up and baled with the CS during harvest. Table 1. Proximate and ultimate analysis of ORG and separated CS. Measurements made using ASTM D7582, ASTM D5373, and ASTM D4239.shows the results from the three materials for comparison, detailing the proximate and ultimate analysis of each fraction. The elemental carbon and moisture content increased more in the LAF than the HAF because of the tissue types and sizes that are preferentially separated into the heavy stream (cob and stalk) after AC. Meanwhile, the elemental oxygen content and volatile content also increased in LAF after AC. On the other hand, the nitrogen and ash content were increased in the HAF after AC. In fact, the LAF fraction from the air classification resulted in a 27 wt. % reduction (from 7.13 wt. % to 5.24 wt. %) in total ash compared with the original as-received CS material, whereby the trend is also in compliance with Lacey et al. [11] and Thompson et al. [2]. The HAF resulted in a higher ash fraction, with 19.10 wt. % total ash that resulted from the higher portion of fines, leaves, and contaminants such as plastic, twine, and introduced dirt typical of harvesting methods. Similar result was also found in other reports in the literature [2]. This indicates a significant reduction in inorganics that are non-convertible and lead to excessive equipment wear [2]. This material beneficiation creates an enhanced feedstock for conversion, but also generates an alternate biomass fraction that requires utilization. As discussed in this work, we investigate HTC as a method of utilization. The conversion and analysis results further considered in this study are focused around the HAF.

As-received corn stover.

Air classified LAF "clean" fraction with fan speed of 1.8 m/s air velocity.

Air classified HAF "dirty" fraction with fan speed of 1.8 m/s air velocity.

Figure 1. Photo of the original (ORG) prepared corn stover (CS) and the air classified separated CS with high ash fraction (HAF) and light ash fraction (LAF) divisions.

Table 1. Proximate and ultimate analysis of ORG and separated CS. Measurements made using ASTM D7582, ASTM D5373, and ASTM D4239.

Sample Name	CS ORG	CS LAF 8 Hz	CS HAF 8 Hz
Moisture (wt. %)	6.5 ± 0.0	6.7 ± 0.0	3.1 ± 0.0
VM (wt. %)	77.2 ± 0.2	78.9 ± 0.1	67.6 ± 0.2
Ash (wt. %)	7.1 ± 0.2	5.2 ± 0.0	19.1 ± 0.1
FC (wt. %)	15.7 ± 0.2	15.9 ± 0.2	13.3 ± 0.1
H (wt. %)	5.5 ± 0.0	5.3 ± 0.4	4.9 ± 0.0
C (wt. %)	46.2 ± 0.1	47.2 ± 0.3	40.4 ± 0.2
N (wt. %)	0.6 ± 0.0	0.5 ± 0.0	1.1 ± 0.0
O (wt. %)	40.4 ± 0.2	41.7 ± 0.2	34.4 ± 0.2
S (wt. %)	0.2 ± 0.0	0.2 ± 0.0	0.2 ± 0.0

3.2. Characterization of Hydrochars Prepared from HAF of CS

HTC experiments were conducted to determine the effect of HTC temperature on the physiochemical properties of hydrochar. Table 2 shows the MY, EY, proximate and ultimate analyses of the ORG CS and hydrochar samples. The MY decreased with the increase in HTC temperature for both ORG and HAF hydrochars. For ORG, the MY was 61.7 ± 3.9 wt. % at HTC200, while it was decreased to 43.1 ± 2.8 wt. % at HTC260. For HAF, the MY was 62.2 ± 1.9 wt. % at HTC200 and then it decreased to 50.1 ± 0.4 wt. % at HTC 260. It was previously reported that MY decreased with increasing HTC temperature [20,22,24]. The attenuation in MY between the lower and higher temperature HTC treatments could be primarily due to the degradation of different components at successively higher temperatures [28]. For example, hemicellulose starts degrading at a lower temperature at approximately 180 °C, cellulose starts breaking down at approximately 230 °C, and the lignin starts decaying significantly with temperatures at and above 260 °C. All these are responsible for the lower MY at higher temperatures [19,24,28,36–38]. Previous studies also suggest that the hydrolysis reaction, which requires the lowest activation energy compared to other decomposition reactions, occurs below 200 °C and results in high MY [36,39]. On the other hand, HTC temperature elevation releases volatile matters, which enhance the dehydration and elimination reactions. This phenomenon takes part in dropping the MY with the increase in HTC temperature [39]. It might be anticipated that the transformation from CS to hydrochars entailed a high proportion of organic degradation, and inorganics solubilization and removal from the solution. It could be possible that when the HTC temperature increased from 200 °C to 260 °C, the dehydration reaction became more prominent than hydrolysis reaction (see Figure 2). The dehydration reaction might synthesize more organic acids (lowering the pH of process liquid), which could potentially catalyze the decomposition of biomass, meaning that more process liquid and gas were being produced and resulted in a low mass yield at high temperatures. Although the MY values at 230 °C for both feedstocks were similar, at 260 °C, HAF showed the highest value. This could be due to the relatively higher content of inorganic dirt and foreign materials in the HAF compared to the ORG.

Table 2. Proximate and ultimate analysis of air classified CS hydrochars. DB is dry basis.

Sample Type	Sample Condition	MY (wt. %)	EY (%)	HHV$_{DB}$ (MJ/kg)	AY (wt. %)	Thermogravimetric Analysis				Ultimate Analysis				
						MC (wt. %)	Ash (wt. %)	VM (wt. %)	FC (wt. %)	C (wt. %)	H (wt. %)	N (wt. %)	S (wt. %)	O (wt. %)
ORG	raw	100.0 ± 0.0	100.0 ± 0.0	18.3 ± 0.2	100.0 ± 0.0	5.9 ± 1.2	5.7 ± 0.9	76.9 ± 0.8	13.3 ± 1.6	45.3 ± 0.9	5.5 ± 0.1	0.6 ± 0.04	BD**	42.8 ± 1.0
	HTC 200	61.7 ± 3.9	66.4 ± 4.2	19.7 ± 0.2	50.4 ± 4.5	1.8 ± 0.0	4.7 ± 0.4	75.5 ± 0.7	17.9 ± 0.7	48.1 ± 0.4	5.7 ± 0.0	0.3 ± 0.1	BD**	41.2 ± 0.4
	HTC 230	54.1 ± 0.6	60.9 ± 0.7	20.7 ± 0.2	72.1 ± 6.4	1.4 ± 0.3	7.6 ± 0.7	69.2 ± 0.8	21.8 ± 1.0	50.9 ± 0.1	5.4 ± 0.1	0.4 ± 0.0	BD**	35.6 ± 0.1
	HTC 260	43.1 ± 2.8	52.0 ± 3.3	22.1 ± 0.2	85.9 ± 11.6	1.2 ± 0.1	11.3 ± 1.6	55.9 ± 0.5	31.6 ± 0.4	55.5 ± 0.0	2.6 ± 2.6	0.5 ± 0.2	BD**	30.0 ± 2.4
LAF	raw	100.0 ± 0.0	100.0 ± 0.0	18.8 ± 0.2	100.0 ± 0.0	5.6 ± 1.6	4.5 ± 0.1	71.2 ± 3.9	17.5 ± 2.2	51.3 ± 0.0	5.5 ± 0.0	0.1 ± 0.0	BD**	38.51 ± 0.0
HAF	raw	100.0 ± 0.0	100.0 ± 0.0	16.8 ± 0.1	100.0 ± 0.0	7.9 ± 0.2	10.3 ± 1.1	64.9 ± 0.4	17.1 ± 0.7	40.6 ± 0.3	5.1 ± 0.2	0.9 ± 0.1	BD**	42.9 ± 0.4
	HTC 200	62.2 ± 1.9	68.9 ± 2.8	18.6 ± 0.2	64.1 ± 3.8	2.3 ± 0.1	10.6 ± 0.6	69.5 ± 0.4	17.6 ± 0.3	43.9 ± 0.2	5.1 ± 0.1	0.9 ± 0.2	BD**	39.4 ± 0.2
	HTC 230	64.9 ± 1.9 *	76.7 ± 2.6	19.9 ± 0.1	67.1 ± 1.3	1.9 ± 0.4	10.6 ± 0.2	66.9 ± 1.5	20.5 ± 1.9	47.5 ± 1.9	4.7 ± 0.3	1.1 ± 0.2	BD**	35.9 ± 1.9
	HTC 260	50.1 ± 0.4 *	66.4 ± 0.4	22.2 ± 0.2	69.7 ± 1.7	1.1 ± 0.2	14.3 ± 0.4	40.3 ± 0.2	44.4 ± 0.0	51.1 ± 0.5	3.5 ± 0.1	1.7 ± 0.2	BD**	29.4 ± 0.5

* values refer to duplicate experiments. All other experiments were triplicated; ** below detection limit.
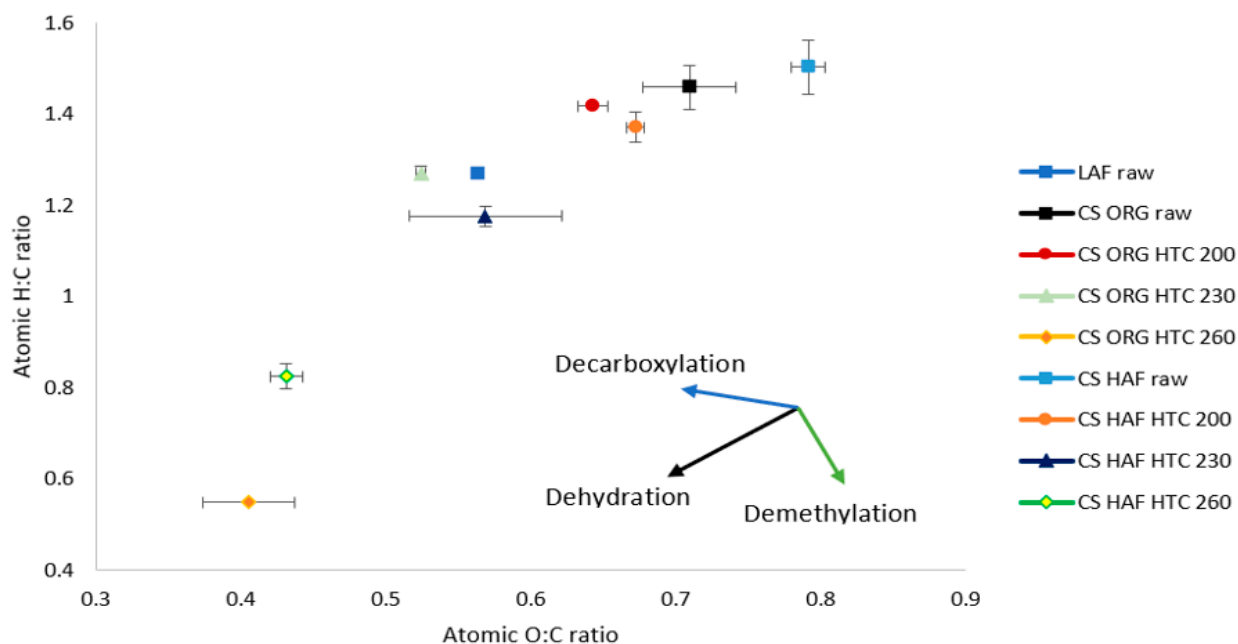
Figure 2. Van-Krevelen diagram.

The AY showed slight changes in their values (Table 2) for HAF hydrochars, but these changes were significant for ORG hydrochars. AY showed remarkable reductions of ~50 wt. % and ~36 wt. % from raw ORG to ORG HTC200 and raw HAF to HAF HTC200, respectively, but it increased for successive HTC temperatures. Qadi et al. [40] and Chen et al. [41] found that HTC aids in the removal of loose minerals from the biomass. One possible explanation is that CS can be accompanied by large amounts of loose dirt during harvesting, depending on method, and this portion was removed significantly during the HTC200 process. It is likely that this agronomic practice contributed to the trapped soil in this sample, as discussed on the previous section. On the other hand, the ORG HTC260 and HAF HTC260 showed the highest AY values of ~86 wt. % and ~70 wt. %, respectively. This could be due to the adsorption of the inorganics from the liquid phase to the solid phase (hydrochar) at elevated temperatures. The oversaturation with minerals in the liquid phase at high temperatures could be responsible for this precipitation phenomenon. Several researchers found that HTC enhances the degradation process with higher temperatures, and produces sugar monomers, furfurals, and organic acids, which leave porous structures of hydrochar. As such, some entrapped/loosely bonded inorganics in the crosslinked matrix might have been adsorbed into the pores of hydrochar during HTC [18,24,40]. Since cellulose and lignin start degrading at around 230 °C and 260 °C, respectively, and create porous structures, they might permit the insoluble inorganics to be absorbed from the process liquid into the hydrochar surface, resulting in higher AY.

The ultimate analysis shown in Table 2 indicates that with the increase in HTC temperature, the carbon content was increased by ~10 wt. % for ORG HTC260 and ~11 wt. % for HAF HTC260 from raw ORG and HAF, respectively, wherein the oxygen content dropped about 13 wt. % and 14 wt. %. Regarding hydrogen, although ORG chars showed essentially no change, HAF chars showed a slight drop (~1.5 wt. %) for HTC 260 from raw HAF. The nitrogen showed insignificant changes in the hydrochars with respect to the feedstock. The higher carbon content and lower oxygen content rationalized the rising HHV with the increase in HTC process temperature. The fuel quality was also analyzed with the van-Krevelen diagram (Figure 2). The van-Krevelen diagram depicts that the closer to the origin of the data the points are, the better the fuel is [33]. The HAF fuel quality was

very low compared to the LAF quality, as expected due to the higher concentration of non-combustible species. Even considering this on an inorganics-free basis, there is a small discrepancy with a lower calorific value in the HAF. As mentioned above, this is attributed to the partitioning of tissues during AC. In addition to having higher inorganics content, these HAF tissues (larger portions of leaf, sheaths) have higher amounts of extractives (cutin resin, protein, etc.). With the increase in HTC temperature, the hydrochar fuel quality (calorific value, and carbon, oxygen, and hydrogen content) increases (up to 32 wt. % in the HAF). Hydrochars produced at 260 °C showed the best fuel quality among all the chars, and this agrees with prior studies undertaken in these condition ranges [5]. As the rise in HTC temperature favored the dehydration and decarboxylation reactions (see Figure 2), this could justify the increase in elemental C and decrease in elemental O content during the carbonization process.

The TGA of the ORG chars showed a decreasing trend (Table 2) of VM and a rising trend of FC. The ORG HTC260 showed ~21 wt. % VM decrease and ~19 wt. % FC increase from the raw ORG, whereas HAF HTC260 showed a significant decrease (~25 wt. %) in VM and increase (~27 wt. %) in FC compared to raw HAF. However, a minimum change in both FC and VM was observed for both feedstocks at 200 °C. Previous studies suggested that the degradation of cellulose at around 220 °C might be responsible for this phenomenon [36,42,43]. Sharma et al. [39] and Titirici et al. [44] further explained cellulose degradation via two routes: (1) cellulose > glucose > 5-hydroxymethyl furfural > carbonized structure; (2) cellulose > aromatic structure. In this study, a possible explanation for receiving higher FC for both ORG and HAF HTC260 is the cellulose carbohydrate's degradation into more carbonaceous particles at successively higher temperatures.

The highest energy content was observed at the 260 °C hydrochars for both ORG and HAF (about 22 MJ/kg), as shown in Table 2, which was almost 4 MJ/kg and 5 MJ/kg higher than with the ORG CS (~18 MJ/kg) and HAF (~17 MJ/kg), respectively. Earlier studies demonstrated that with the increasing HTC temperature, the HHV and corresponding EY showed upward and downward trends, respectively [20,22,24]. The EY reported in Table 2 showed a descending trend for ORG chars, but a more complex pattern for HAF hydrochars. A possible explanation for the discrepancies between the hydrochar EY values is that the HAF HTC230 had higher MY, which could be due to the retention of cellulose in the hydrochar due to partial degradation. In addition, the enriched energy content and mass yield is convolved with the reduction in inorganics to create a potentially complex optimization for the energy yield of the HAF.

3.3. Energy Recovery by Integrating AC–HTC Process

Figure 3 shows three different proposed scenarios: the AC-only process, the HTC-only process, and the integrated AC–HTC process. The main objective of these processes was to determine the energy recovery from CS. For all processes, the basis was arbitrarily taken as 100 kg dry ORG feed. In the AC-only process, the throughputs were LAF and HAF, as the below-screen particles were assumed to be negligible. The HAF was considered as waste and discarded from the process for AC. The LAF was the only throughput that was pelletized and the HHV was determined. In the HTC-only process, dry ORG was directly fed into the HTC reactor at three different temperatures (200, 230, and 260 °C), and then corresponding hydrochars were pelletized to find out the energy recovery of the HTC process. The last process was considered as the integrated AC–HTC process, which comprised the AC followed by the HTC process. As mentioned earlier, the AC process had two main throughputs: LAF and HAF. The HAF waste was fed into the HTC process at three different temperatures (200, 230, and 260 °C). The hydrochars were then mixed with LAF at their corresponding weight ratios and pelletized to find out the energy recovery from the integrated process.
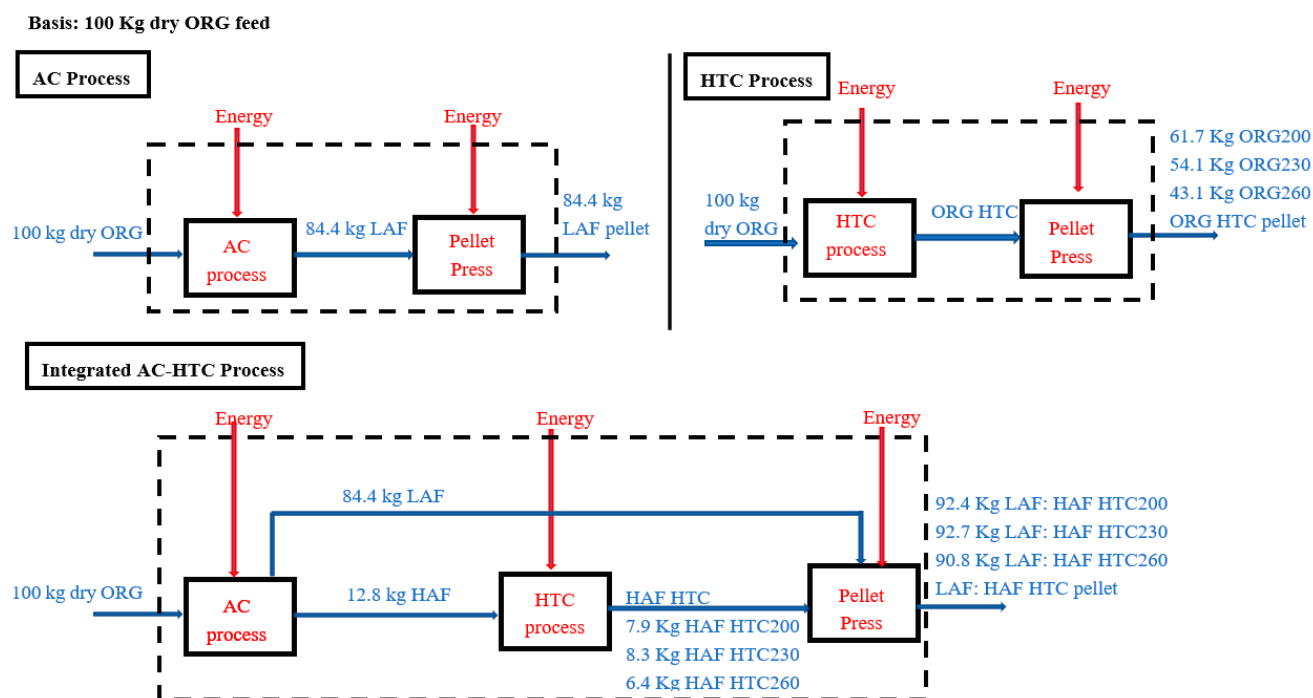
Figure 3. AC, HTC, and integrated AC–HTC process.

The overall energy balances for the three scenarios were calculated using Equation (6)–(11). For process units, the specific energy consumptions (SECs) were found from [45,46] and shown in Table 3. Specific energy consumption for each process unit. The SEC of AC was calculated as 0.0036 MJ/kg by INL and the basis was taken as per kg dry LAF. The pellet press SEC was found to be 0.4 MJ/kg dry feed for the raw LAF and LAF–HTC mixtures and 0.2 MJ/kg dry hydrochar for the ORG chars [45]. Earlier, it was demonstrated that the pellet press SEC increases with a higher feed rate, feed moisture (wt. %), and length-to-diameter (L/D) ratio of pellet die, etc. [47]. For example, the moisture (wt. %) in the biomass feed is higher than in the hydrochar feed due to the higher hydrophilicity [48], which can increase the overall SEC of biomass pelletization. Here, the SEC for biomass and biomass–hydrochar mixtures under pelletization (Table 3. Specific energy consumption for each process unit) was considered higher than the hydrochar SEC due to the higher feed, moistures (wt. %), and/or L/D ratio. For the case of SEC of HTC, the required SEC was found to be 5.9, 6.3, and 6.7 MJ/kg dry feed for HTC200, HTC230, and HTC260, respectively (for both ORG and HAF chars) [46]. As higher temperatures require higher energy consumption [46], HTC260 has the highest SEC (6.7 MJ/kg dry feed) among all the chars. Table 4 shows the overall energy balance of the processes.

As per the AC process (Table 4), the overall net energy in was 1833.6 MJ (Equations (6), (7), and (11) and Table 4) and the energy out was 1588.3 MJ (Equation (8), Table 4). The recoverable energy of the HAF was found by the difference between the ORG and LAF energies, which was ~245 MJ (Equation (9), Table 4). Since the HAF waste was not processed and eliminated after AC, the recoverable energy was 0 MJ for the AC-only

In the case of the HTC-only process (Table 4), the overall energy in was 2439.6 MJ, 2474.1 MJ, and 2507.9 MJ for ORG HTC200, 230 and 260, respectively (Equations (6), (7) and Table 4). The overall energy out was 1217.6 MJ, 1116.4 MJ and 953.8 MJ for HTC200, 230 and 260, respectively (Equation (8) and Table 4). The energy consumptions for the bulk quantity of HTC of ORG significantly elevated the process' overall energy demand. Since the HTC process was highly energy-intensive, the energy recovery was not feasible. process.

Table 3. Specific energy consumption for each process unit.

Process Units	Specific Energy Consumption (SEC)	Unit	Reference Paper
AC	0.0036	MJ/kg dry LAF	This study
Pellet press for LAF	0.4	MJ/kg dry feed	[45]
HTC for ORG200	5.9	MJ/kg dry feed	[46]
HTC for ORG230	6.3	MJ/kg dry feed	[46]
HTC for ORG260	6.7	MJ/kg dry feed	[46]
Pellet press for ORG200	0.2	MJ/kg dry hydrochar	[45]
Pellet press for ORG230	0.2	MJ/kg dry hydrochar	[45]
Pellet press for ORG260	0.2	MJ/kg dry hydrochar	[45]
HTC for HAF200	5.9	MJ/kg dry feed	[46]
HTC for HAF230	6.3	MJ/kg dry feed	[46]
HTC for HAF260	6.7	MJ/kg dry feed	[46]
Pellet press for LAF:HAF HTC200	0.4	MJ/kg dry feed	[45]
Pellet press for LAF:HAF HTC230	0.4	MJ/kg dry feed	[45]
Pellet press for LAF:HAF HTC260	0.4	MJ/kg dry feed	[45]

Table 4. Energy extracted from HAF waste.

Process Type	HTC	Energy in (MJ)				Energy out (MJ)			Potential Energy (MJ) in HAF Waste	Energy Recovery (MJ) from HAF Waste
		ORG Feed	AC	HTC of HAF	Pellet Press	LAF Pellet	ORG Pellet	LAF:HAF HTC Pellet		
AC Process		1833.3	0.3	-	37.1	1588.3		-	245.0	0
HTC Process	ORG HTC 200	1833.3	-	594.0	12.3	-	1217.6	-	245.0	-
	ORG HTC 230	1833.3	-	630.0	10.8	-	1116.4	-	245.0	-
	ORG HTC260	1833.3	-	666.0	8.6	-	953.8	-	245.0	-
Integrated AC–HTC Process	LAF: HAF HTC200	1833.3	0.3	76.0	40.6	-	-	1736.5	245.0	68.7
	LAF: HAF HTC230	1833.3	0.3	80.6	40.8	-	-	1752.6	245.0	80.0
	LAF: HAF HTC260	1833.3	0.3	85.3	40.0	-	-	1727.4	245.0	51.0

As per the integrated AC–HTC process (Table 4), the HAF waste was hydrothermally carbonized to utilize the recoverable energy present (~245 MJ) in the product, and further mixed with the LAF stream for taking advantage of AC preprocessing (Equation (10), and Table 4). The results in Table 4 show that the energy recovery was the maximum (~80 MJ) for LAF:HAF under HTC230, which was about ~11 MJ and ~29 MJ higher than LAF:HAF HTC200 and LAF:HAF HTC260, respectively (using Equations (6)–(8), (10), (11), and Table 4). The higher FC and elemental carbon for HAF HTC230 than HAF HTC200 could contribute as a better solid fuel compared to LAF: HAF HTC200. On the other hand, although HAF HTC260 has higher FC and elemental carbon than HAF HTC230, due to the higher volatile matters as well as the elemental oxygen in HAF HTC230, this could enhance the energy content of the LAF:HAF HTC230. Since volatiles are mainly made of short chain hydrocarbons, long chain hydrocarbons and aromatic hydrocarbons that are easy to distill off, it might be possible that the heavier hydrocarbons break into lighter gases during combustion and react with limited oxygen via partial oxidation, releasing more

energy as heat [49]. In this context, integrating the LAF and HAF HTC230 process streams might give a better energy recovery out of the AC reject stream. Moreover, in this mode, the HTC process energy consumptions were significantly less than the HTC-only mode, which might impact the overall energy recovery in a positive dimension. On the other hand, the final product energy value was much higher than the AC-only mode, which bears the importance of combining the AC and HTC processes together. Overall, the integrated AC–HTC could become a better option to take the advantage of the potential waste energy as valuable utilizable energy, and minimize the overall energy lost.

Equations used:

$$\text{Energy in (MJ) of feed} = \text{HHV of feed} \times \text{Total mass of feed} \tag{6}$$

$$\text{Energy in (MJ) of process unit} = \text{Specific energy consumption of} \\ \text{the unit} \times \text{Total mass of feed or product} \tag{7}$$

$$\text{Energy out (MJ) of product} = \text{HHV} \times \text{Total mass of product} \tag{8}$$

$$\text{Potential energy (MJ) in HAF waste} = \text{LAF pellet-ORG feed} \tag{9}$$

$$\text{Energy recovery (MJ) from HAF waste for the integrated AC-HTC process} \\ = \text{LAF:HAF HTC pellet-HTC of HAF-pellet press for LAF:HAF HTC} \\ \text{pellet-net energy of LAF pellet} \tag{10}$$

$$\text{Net energy (MJ) of LAF pellet} = \text{LAF pellet-Pellet press for LAF} \tag{11}$$

4. Conclusions

This study investigated an integrated AC–HTC process to recover the energy from corn stover. An air classifier was used to beneficiate CS into a purified biomass stream with 27 wt. % reduction in ash content from LAF with 84.4 wt. % mass recovery. The waste from this fractionation technique was used as a feedstock for HTC to produce a high-energy fuel pellet (19–22 MJ/kg). When CS was hydrothermally carbonized, both MY and AY were decreased with the HTC temperature; meanwhile, the energy content of the hydrochar was increased. This study showed that the AC and HTC processes cannot recover any energy from the HAF stream individually. On the other hand, along with the high-energy densified hydrochar, the integrated AC–HTC process further showed significant energy recovery (~800 MJ/tonne) from the HAF. Therefore, this study provides evidence of an HTC that can be integrated with AC to reduce the inorganic content and recover energy. Adopting HTC with AC could potentially transform CS into an advanced biorefinery feedstock, while still utilizing the otherwise lost organics from the AC process. Further sustainability and technoeconomic assessment of AC and HTC are needed to justify the economic viability of the integrated process. However, the energy consumption of this study was calculated based on the laboratory-scale data, which could vary at a large scale. Process economics with large-scale data could reveal additional data that might assist technology maturation.

Informed Consent Statement: Not applicable.

Data Availability Statement: Not applicable.

References

1. *U.S. Billion-Ton Update: Biomass Supply for a Bioenergy and Bioproducts Industry*; U.S. Department of Energy, Energy Efficiency and Renewable Energy, Office of the Biomass Program: Washington, DC, USA, 2011; p. 235.
2. Thompson, V.S.; Lacey, J.A.; Hartley, D.; Jindra, M.A.; Aston, J.E.; Thompson, D.N. Application of air classification and formulation to manage feedstock cost, quality and availability for bioenergy. *Fuel* **2016**, *180*, 497–505. [CrossRef]
3. Perlack, R.D.; Wright, L.L.; Turhollow, A.F.; Graham, R.L.; Stokes, B.J.; Erbach, D.C. *Biomass as Feedstock for a Bioenergy and Bioproducts Industry: The Technical Feasibility of a Billion-Ton Annual Supply*; Oak Ridge National Laboratory: Oak Ridge, TN, USA, 2005; p. 1216415. [CrossRef]
4. Zhichao, W.; Dunn, J.B.; Wang, M.Q. *Updates to the Corn Ethanol Pathway and Development of an Integrated Corn and Corn Stover Ethanol Pathway in the GREET™ Model*; No. ANL/ESD-14/11; Argonne National Lab. (ANL): Argonne, IL, USA, 2014.
5. Machado, N.; Castro, D.; Queiroz, L.; Santos, M.; Costa, C. Production and Characterization of Energy Materials with Adsorbent Properties by Hydrothermal Processing of Corn Stover with Subcritical H_2O. *J. Appl. Solut. Chem. Model.* **2016**, *5*, 117–130. [CrossRef]
6. Kim, S.; Dale, B.E. Global potential bioethanol production from wasted crops and crop residues. *Biomass Bioenergy* **2004**, *26*, 361–375. [CrossRef]
7. Zhang, Y.; Jiang, Q.; Xie, W.; Wang, Y.; Kang, J. Effects of temperature, time and acidity of hydrothermal carbonization on the hydrochar properties and nitrogen recovery from corn stover. *Biomass Bioenergy* **2019**, *122*, 175–182. [CrossRef]
8. Biswas, B.; Pandey, N.; Bisht, Y.; Singh, R.; Kumar, J.; Bhaskar, T. Pyrolysis of agricultural biomass residues: Comparative study of corn cob, wheat straw, rice straw and rice husk. *Bioresour. Technol.* **2017**, *237*, 57–63. [CrossRef]
9. Emerson, R.M.; Hernandez, S.; Williams, C.L.; Lacey, J.A.; Hartley, D.S. Improving bioenergy feedstock quality of high moisture short rotation woody crops using air classification. *Biomass Bioenergy* **2018**, *117*, 56–62. [CrossRef]
10. Williams, C.L.; Emerson, R.M.; Hernandez, S.; Klinger, J.L.; Fillerup, E.P.; Thomas, B.J. Preprocessing and hybrid biochemical/thermochemical conversion of short rotation woody coppice for biofuels. *Front. Energy Res.* **2018**, *6*, 74. [CrossRef]
11. Lacey, J.A.; Aston, J.E.; Westover, T.L.; Cherry, R.S.; Thompson, D.N. Removal of introduced inorganic content from chipped forest residues via air classification. *Fuel* **2015**, *160*, 265–273. [CrossRef]
12. Reza, M.T.; Emerson, R.; Uddin, M.H.; Gresham, G.; Coronella, C.J. Ash reduction of corn stover by mild hydrothermal preprocessing. *Biomass Convers. Biorefinery* **2014**. [CrossRef]
13. Humbird, D.; Davis, R.; Tao, L.; Kinchin, C.; Hsu, D.; Aden, A. *Process Design and Economics for Biochemical Conversion of Lignocellulosic Biomass to Ethanol: Dilute-Acid Pretreatment and Enzymatic Hydrolysis of Corn Stover*; Technical Report NREL/TP-5100-47764; National Renewable Energy Lab. (NREL): Golden, CO, USA, 2011; p. 1013269.
14. Möller, M.; Nilges, P.; Harnisch, F.; Schröder, U. Subcritical Water as Reaction Environment: Fundamentals of Hydrothermal Biomass Transformation. *ChemSusChem* **2011**, *4*, 566–579. [CrossRef]
15. Brunner, G. Heat Transfer. In *situ Spectroscopic Techniques at High Pressure*; Elsevier: Amsterdam, The Netherlands, 2014; Volume 5, pp. 227–263. [CrossRef]
16. Öztürk, I.; Irmak, S.; Hesenov, A.; Erbatur, O. Hydrolysis of kenaf (*Hibiscus cannabinus* L.) stems by catalytical thermal treatment in subcritical water. *Biomass Bioenergy* **2010**, *34*, 1578–1585. [CrossRef]
17. Machado, N.; De Castro, D.; Santos, M.; Araújo, M.; Lüder, U.; Herklotz, L.; Werner, M.; Mumme, J.; Hoffmann, T. Process analysis of hydrothermal carbonization of corn Stover with subcritical H_2O. *J. Supercrit. Fluids* **2018**, *136*, 110–122. [CrossRef]
18. Funke, A.; Ziegler, F. Hydrothermal carbonization of biomass: A summary and discussion of chemical mechanisms for process engineering. *Biofuels Bioprod. Biorefin.* **2010**, *4*, 160–177. [CrossRef]
19. Minaret, J.T. *Hydrothermal Carbonization of Corn Residuals to Produce a Solid Fuel Replacement for Coal*; The University of Guelph: Keiu Lake, ON, Canada, 2015; p. 133.
20. Kobayashi, N.; Okada, N.; Hirakawa, A.; Sato, T.; Kobayashi, J.; Hatano, S.; Itaya, Y.; Mori, S. Characteristics of Solid Residues Obtained from Hot-Compressed-Water Treatment of Woody Biomass. *Ind. Eng. Chem. Res.* **2009**, *48*, 373–379. [CrossRef]
21. Lynam, J.G.; Coronella, C.J.; Yan, W.; Reza, M.T.; Vasquez, V.R. Acetic acid and lithium chloride effects on hydrothermal carbonization of lignocellulosic biomass. *Bioresour. Technol.* **2011**, *102*, 6192–6199. [CrossRef] [PubMed]
22. Yan, W.; Acharjee, T.C.; Coronella, C.J.; Vásquez, V.R. Thermal pretreatment of lignocellulosic biomass. *Environ. Prog. Sustain. Energy* **2009**, *28*, 435–440. [CrossRef]
23. Hoekman, S.K.; Broch, A.; Robbins, C. Hydrothermal Carbonization (HTC) of Lignocellulosic Biomass. *Energy Fuels* **2011**, *25*, 1802–1810. [CrossRef]

24. Reza, M.T.; Lynam, J.G.; Uddin, M.H.; Coronella, C.J. Hydrothermal carbonization: Fate of inorganics. *Biomass Bioenergy* **2013**, *49*, 86–94. [CrossRef]

25. Tu, R.; Sun, Y.; Wu, Y.; Fan, X.; Wang, J.; Cheng, S.; Jia, Z.; Jiang, E.; Xu, X. Improvement of corn stover fuel properties via hydrothermal carbonization combined with surfactant. *Biotechnol. Biofuels* **2019**, *12*, 1–19. [CrossRef]

26. Wang, T.; Zhai, Y.; Zhu, Y.; Li, C.; Zeng, G. A review of the hydrothermal carbonization of biomass waste for hydrochar formation: Process conditions, fundamentals, and physicochemical properties. *Renew. Sustain. Energy Rev.* **2018**, *90*, 223–247. [CrossRef]

27. Wu, Q.; Yunqiao, P.; Hao, N.; Wells, T.; Meng, X.; Li, M.; Pu, Y.; Liu, S.; Ragauskas, A.J. Characterization of products from hydrothermal carbonization of pine. *Bioresour. Technol.* **2017**, *244*, 78–83. [CrossRef] [PubMed]

28. Smith, A.M.; Singh, S.; Ross, A.B. Fate of inorganic material during hydrothermal carbonisation of biomass: Influence of feedstock on combustion behaviour of hydrochar. *Fuel* **2016**, *169*, 135–145. [CrossRef]

29. Wagner, W.; Pruß, A. The IAPWS Formulation 1995 for the Thermodynamic Properties of Ordinary Water Substance for General and Scientific Use. *J. Phys. Chem. Ref. Data* **2002**, *31*, 387–535. [CrossRef]

30. Archers, D.G.; Wang, P. The Dielectric Constant of Water and Debye-HOckel Limiting Law Slopes. *J. Phys. Chem. Ref. Data* **1990**, *19*, 41.

31. Bandura, A.V.; Lvov, S.N. The Ionization Constant of Water over Wide Ranges of Temperature and Density. *J. Phys. Chem. Ref. Data* **2006**, *35*, 15–30. [CrossRef]

32. Kaliyan, N.; Morey, R.V. Densification Characteristics of Corn Stover and Switchgrass. *Trans. ASABE* **2009**, *52*, 907–920. [CrossRef]

33. Saba, A.; Saha, P.; Reza, M.T. Co-Hydrothermal Carbonization of coal-biomass blend: Influence of temperature on solid fuel properties. *Fuel Process. Technol.* **2017**, *167*, 711–720. [CrossRef]

34. Saha, N.; Xin, D.; Chiu, P.C.; Reza, M.T. Effect of Pyrolysis Temperature on Acidic Oxygen-Containing Functional Groups and Electron Storage Capacities of Pyrolyzed Hydrochars. *ACS Sustain. Chem. Eng.* **2019**, *7*, 8387–8396. [CrossRef]

35. Thompson, V.S.; Aston, J.E.; Lacey, J.A.; Thompson, D.N. Optimizing Biomass Feedstock Blends with Respect to Cost, Supply, and Quality for Catalyzed and Uncatalyzed Fast Pyrolysis Applications. *BioEnergy Res.* **2017**, *10*, 811–823. [CrossRef]

36. Libra, J.A.; Ro, K.S.; Kammann, C.; Funke, A.; Berge, N.D.; Neubauer, Y.; Titirici, M.-M.; Fühner, C.; Bens, O.; Kern, J.; et al. Hydrothermal carbonization of biomass residuals: A comparative review of the chemistry, processes and applications of wet and dry pyrolysis. *Biofuels* **2011**, *2*, 71–106. [CrossRef]

37. Pastor-Villegas, J.; Pastor-Valle, J.; Rodríguez, J.M.; García, M.G. Study of commercial wood charcoals for the preparation of carbon adsorbents. *J. Anal. Appl. Pyrolysis* **2006**, *76*, 103–108. [CrossRef]

38. Kumar, S.; Gupta, R.; Lee, Y.; Gupta, R.B. Cellulose pretreatment in subcritical water: Effect of temperature on molecular structure and enzymatic reactivity. *Bioresour. Technol.* **2010**, *101*, 1337–1347. [CrossRef] [PubMed]

39. Sharma, R.; Jasrotia, K.; Singh, N.; Ghosh, P.; Srivastava, S.; Sharma, N.R.; Singh, J.; Kanwar, R.; Kumar, A. A Comprehensive Review on Hydrothermal Carbonization of Biomass and Its Applications. *Chem. Afr.* **2019**, *3*, 1–19. [CrossRef]

40. Qadi, N.; Takeno, K.; Mosqueda, A.; Kobayashi, M.; Motoyama, Y.; Yoshikawa, K. Effect of Hydrothermal Carbonization Conditions on the Physicochemical Properties and Gasification Reactivity of Energy Grass. *Energy Fuels* **2019**, *33*, 6436–6443. [CrossRef]

41. Chen, S.-F.; Mowery, R.A.; Scarlata, C.J.; Chambliss, C.K.; Chambliss, K. Compositional Analysis of Water-Soluble Materials in Corn Stover. *J. Agric. Food Chem.* **2007**, *55*, 5912–5918. [CrossRef]

42. Saha, N.; Saba, A.; Reza, M.T. Effect of hydrothermal carbonization temperature on pH, dissociation constants, and acidic functional groups on hydrochar from cellulose and wood. *J. Anal. Appl. Pyrolysis* **2019**, *137*, 138–145. [CrossRef]

43. Peterson, A.A.; Vogel, F.; Lachance, R.P.; Fröling, M.; Antal, J.M.J.; Tester, J.W. Thermochemical biofuel production in hydrothermal media: A review of sub- and supercritical water technologies. *Energy Environ. Sci.* **2008**, *1*, 32–65. [CrossRef]

44. Titirici, M.M.; Thomas, A.; Yu, S.-H.; Müller, A.J.-O.; Antonietti, M. A Direct Synthesis of Mesoporous Carbons with Bicontinuous Pore Morphology from Crude Plant Material by Hydrothermal Carbonization. *Chem. Mater.* **2007**, *19*, 4205–4212. [CrossRef]

45. Tumuluru, J.S. High moisture corn stover pelleting in a flat die pellet mill fitted with a 6 mm die: Physical properties and specific energy consumption. *Energy Sci. Eng.* **2015**, *3*, 327–341. [CrossRef]

46. Lucian, M.; Fiori, L. Hydrothermal Carbonization of Waste Biomass: Process Design, Modeling, Energy Efficiency and Cost Analysis. *Energies* **2017**, *10*, 211. [CrossRef]

47. Tumuluru, J.S. Specific energy consumption and quality of wood pellets produced using high-moisture lodgepole pine grind in a flat die pellet mill. *Chem. Eng. Res. Des.* **2016**, *110*, 82–97. [CrossRef]

48. Reza, M.T.; Lynam, J.G.; Vasquez, V.R.; Coronella, C.J. Pelletization of biochar from hydrothermally carbonized wood. *Environ. Prog. Sustain. Energy* **2012**, *31*, 225–234. [CrossRef]

49. Wang, T. An overview of IGCC systems. In *Integrated Gasification Combined Cycle (IGCC) Technologies*; Wang, T., Stiegel, G., Eds.; Woodhead Publishing: Cambridge, UK, 2017; pp. 1–80. [CrossRef]